Small 2 (2006), 230 - 234

Surface-Charge-Induced Reversible Phase Transitions of Bi Nanoparticles[+]

Jakob B. Wagner*, Marc-Georg Willinger, Jens-Oliver Müller, Dang Sheng Su*, Robert Schlögl,

Fritz-Haber-Institut der Max-Planck-Gesellschaft, Faradayweg 4-6, 14195 Berlin, Germany, Fax: (+49) 30-8413-4401

[*]Correspondence to Jakob B. Wagner, Fritz-Haber-Institut der Max-Planck-Gesellschaft, Faradayweg 4-6, 14195 Berlin, Germany, Fax: (+49) 30-8413-4401, Email: (wagner_j@fhi-berlin.mpg.de)

[*]Correspondence to Dang Sheng Su, Fritz-Haber-Institut der Max-Planck-Gesellschaft, Faradayweg 4-6, 14195 Berlin, Germany, Fax: (+49) 30-8413-4401, Email: (dangsheng@fhi-berlin.mpg.de)

[+]This work was partly supported by SFB-546 of the Deutsche Forschungsgemeinschaft.

electron microscopy, nanoparticles, phase transitions, surface charge

Much of the interest in nanostructured materials originates from the challenge to find materials with properties that are substantially different from those of the same materials on a larger scale. New dielectric, [1] ferromagnetic, [2] catalytic, [3] and other properties are indeed being realized. Of particular interest are nanoparticles that exist in new structures, metastable structures, or known structures extended beyond the composition or stability ranges of ordinary bulk materials.

Transmission electron microscopy (TEM) is an important tool for characterization of nanosized particles, either free standing on a support or dispersed in a matrix. Its ability to combine images with diffraction and chemical microanalysis on well-defined areas or in volumes is a unique combination of information in real space and reciprocal space, on the one hand, and on elastic and inelastic interactions, on the other. Together, these techniques lead to a sound knowledge of the material structure at the morphological, crystallographic, and chemical levels.

However, besides these capabilities and advantages, it should not be forgotten that electron microscopy proceeds from the interaction of fast, energetic electrons with the sample and that the energy exchanged may sometimes cause significant perturbations in the system under observation, ranging from chemical-bond breaking to excitation of electronic levels or collective charge oscillations, atom ionization, and even to irreversible atom displacement by knock-on.[4] In that sense, TEM samples in an electron beam are in a state far from equilibrium.[5] The electron-beam-induced perturbations of the system can be used to manipulate nanostructures by controlling the properties of the focused electron beam. The combination of an electron beam as a nanoprobe and a nanotool has previously been used to produce diamonds from onion-like carbon[6], [7] and for measuring the electric, mechanical, and field-emission properties of carbon nanotubes.[8]

Here we report on the direct imaging of reversible phase transitions observed in nanometer-sized Bi particles induced by surface charging under controlled electron-beam intensities. The spatially confined Bi particles are observed to undergo fast recrystallizations under the electron beam irradiation. A similar instability of nanoparticles observed in electron microscopy has been reported previously for Bi, [9] Au, [10]-[12] Pd and In, [13] and Pb.[14] Under more extreme conditions (increased electron current density) the Bi particles melt. However, for very high current densities the Bi particles solidify and high-frequency fluctuations similar to the case of lower current density are observed. Superheating of embedded low-dimensional materials is a

known phenomenon,[15] but to our knowledge it has never been reported for free supported particles.

The phenomena described below are, in general, observed for the Bi nanoparticles supported on all the three different substrates used in the present work (VPO (vanadium phosphorus oxide catalyst material promoted with Bi), [16] C-films, and Bi agglomerates) in the same electron beam intensity range. The study of the fluctuations is based on a large series of observations.

The nanoparticles were observed at a high magnification that is suitable for lattice fringe imaging. It is possible to reveal lattice fringes in the Bi particles by using a very low electron current density ($\approx 5.0\times10^{3}$ A m^{-2}). However, the crystalline structures are fluctuating rapidly. Snapshots were therefore acquired with the CCD camera using a short acquisition time (see Figure1a).

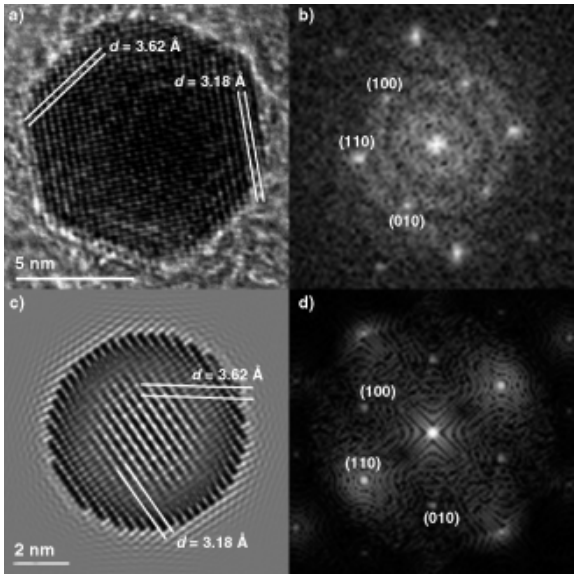

Figure 1. a) Lattice fringe images of a particle supported on a carbon film. b) Fast Fourier transformation (FFT) of the image shown to the left. The measured lattice fringe distances and their mutual angles coincide with the calculated ones found for crystalline bismuth oriented in the [001] direction. c) HRTEM simulation of a 7.5-nm spherical Bi particle at Scherzer defocus (-60 nm). d) FFT of the simulated image shown in (c).

The clearly faceted particle shown in Figure 1 a and b reveals the (100), (010), and (110) planes of rhombohedral bismuth. Although the {100} reflections are kinetically forbidden, high-resolution TEM (HRTEM) simulations of Bi particles show that these planes are indeed revealed when using the dynamical multi-slice approach (Figure 1 c and d). The HRTEM simulations were performed with the RHODIUS[17] and EMS[18] software packages.

Structural rearrangements of Bi clusters prepared by Bi deposition directly on amorphous carbon microscope grids[9], [19] were previously reported as being due to rotations around the zone axis.[19] However, in the present studies the zone axis of the crystalline Bi particles is observed to change during the structural fluctuations (see Figure 2).

Figure 3 shows the development of a Bi particle supported on the carbon film as the electron beam intensity is increased. Figure 3 a shows the crystalline phase of Bi observed at low current density ($<6\times10^{3}$ A m^{-2}) viewed along the [$11\bar{1}$] zone-axis, where (011) and (101) lattice fringes are revealed. Increasing the electron beam intensity results in an apparent melting of the particles (Figure 3 b): the particles no longer reveal lattice fringes and become small, spherical droplets. The projected area of the nanoparticles seems to be conserved, thereby indicating that the particles do not wet the support. Increasing the beam intensity even more ($>4\times10^{5}$ A m^{-2}) results

in yet another phase transition. The particles reveal lattice fringes again and become clearly faceted. The lattice fringes shown in Figure 3 c are those of the $\{10\bar{1}\}$ family corresponding to the $[1\bar{1}\,1]$ zone axis. Flickering is also observed in this state the due to fast reorientations, melting, and resolidification of the crystals. The lattice constant of the Bi particles in the high current density regime was found to be identical to the lattice constant in the low current density regime. The observed phase transitions are both reversible, with no apparent hysteresis as the electron beam intensity is varied.

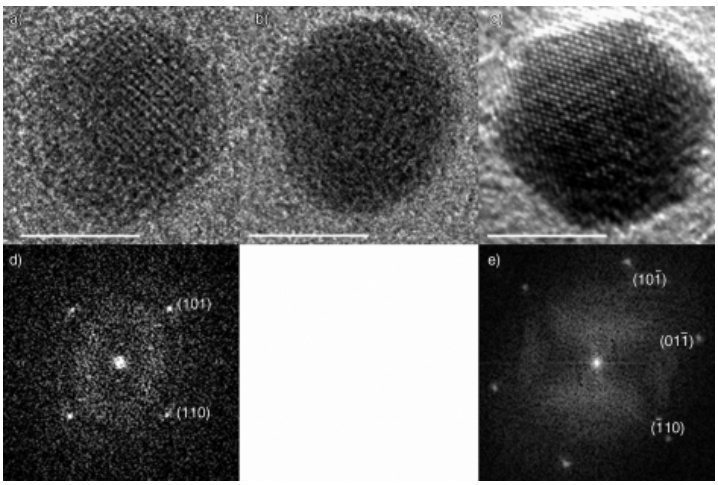

Figure 3. Development of a Bi particle supported on an amorphous carbon film with increasing current density: a) low current density, crystalline phase; b) medium current density, liquid phase; c) high current density, the Bi particle recrystallizes; d) FFT of particle shown in (a); e) FFT of particle shown in (c). Scale bars measure 5 nm. The transformations are reversible.

As the Bi particles melt the apparent interface area remains constant, as shown in Figure 3 and in a profile view of the supported Bi particles shown in Figure 4. The profile views shown in Figure 4 were acquired from Bi particles supported on VPO.

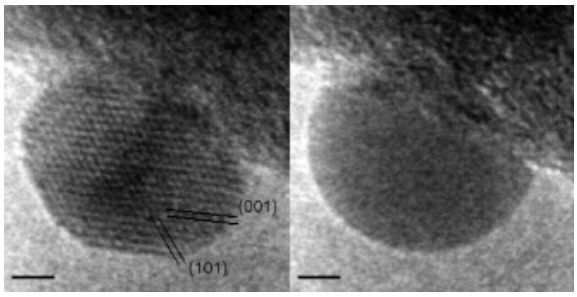

Figure 4. Profile view of a Bi particle supported on VPO showing the solid and liquid phase at current densities below and above 6×10^3 A m^{-2}, respectively. The scale bar measures 2 nm

Inelastic scattering of incoming electrons by the atomic electrons that surround the nucleus might cause the specimen to become charged if low-electric-conducting materials are probed. The energy deposited from the incoming electron beam will increase the temperature of the sample locally, leading to a possible melting for materials with a low melting temperature such as bismuth. As the melting temperature, in general, decreases for decreasing dimensions of the nanoparticles, the effective melting temperature of the probed Bi particles is considerable lower than that of the bulk material.[20]-[22] In situ heating of the support to 400 K with a heating holder results in liquid Bi particles independent of the electron beam intensity. Another aspect of the small size of the Bi particles is their relatively high surface area, which makes the influence of the surface tension large enough to change the effective melting temperature.[23]

The crystalline fluctuations observed in the Bi particles at low electron-beam intensity might be caused by a poor thermal contact between the Bi particle and the support. The electron beam heats the Bi nanocrystal and induces the melting. The thermal contact between liquid Bi and the support is higher than the thermal contact between solid Bi and support, therefore the heat is lost to the support and the particle recrystallizes. These events can occur many times per second.[19] This hypothesis can be summarized as shown in Figure 5 a. In general, the Bi particles have to be treated with an intense electron beam for some minutes in order to activate the structural fluctuations.

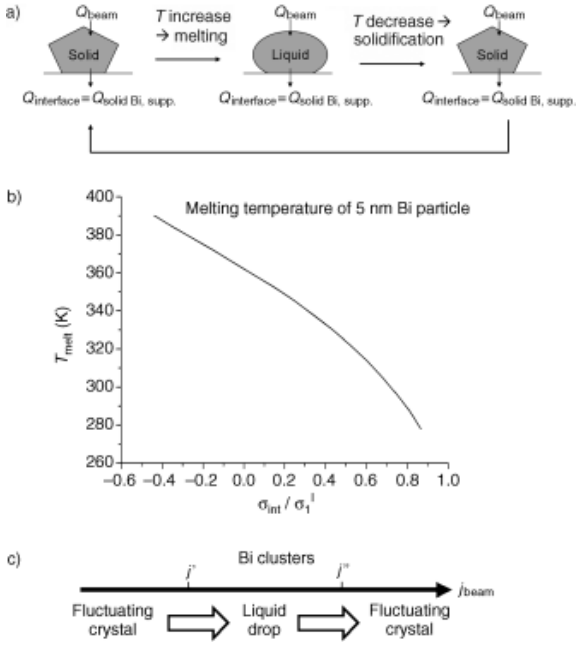

Figure 5. a) Schematic view of the fluctuation of the Bi particles. b) The melting temperature of a 5-nm Bi particle as a function of the Bi/support interface energy. σ_{int} denotes the interface energy between liquid Bi and the support, σ_1^l denotes the surface energy of liquid Bi. c) Phase of the Bi clusters as function of electron-beam current density (j'=6×10^3 A m^{-2}; j''=4×10^5 A m^{-2}).

When the heat induced by the electron beam in the Bi particle becomes greater than the heat flow from the liquid Bi particle to the support (upon increasing the electron beam intensity), the Bi particle stays liquid as the temperature does not decrease below the solidification temperature.

Bulk Bi is known to be a semi-metal (poor conductor) as the total density of electrons at the Fermi surface is about a factor of 10^5 lower in Bi than in a typical metal.[24], [25] Charging of materials in TEM is mostly due to Auger electrons, as described by Cazaux, [26] as they have sufficient energy to overcome the attracting field from the ionized atoms. In general, the irradiated area is discharged by charge flow from the surrounding material. For the present system the charge flow has an upper limit, which leads to a charging of the Bi particles when the probability of ionization per unit time is increased due to a higher electron current density. The Bi will discharge when the electron current density, and thereby the probability of ionization per unit time, is decreased. Charging of surfaces and interfaces due to irradiation in transmission electron microscopy has been treated in detail.[26] From ab initio calculations it is known that the charging of surfaces and interfaces induces changes in the surface and interface energy.[27], [28]

The melting temperature has been shown to be dependent on the contact angle of supported particles from a first-approach model developed by Storozhev.[23] As the contact angle is related to the interface energy between the particle and the substrate, a charge build-up at the particle/substrate interface will alter the interface energy and thereby change the melting

temperature of the system. This first- approach model considers the particles as spheres (both as solid and liquid) and considers a geometrical minimization based on the surface energies of the solid and liquid phases, respectively. Using this model, [23] the melting temperature for a 5-nm Bi particle was calculated as a function of the interface energy between the substrate and particle. The result is shown in Figure 5 b, where it can be seen that realistic changes in the interface energy can account for a difference of more than 100 K in the melting temperature. The magnitude of the electric fields arising from charged areas due to electron beams, calculated by Cazaux and Egerton, [5], [26] gives rise to significant changes in the surface and interface energies that are large enough to alter the melting temperature.

Due to the increased melting temperature of the Bi particles in the high current density case, the situation is similar to the low current density case and the temperature of the Bi particles oscillates around the new melting temperature of the Bi particles. The phase transitions are fully reversible both in the low-dose regime and the high-dose regime. Furthermore, the phase transitions are observed with different supports (with different electric and thermal properties) for the Bi particles, thus indicating that the phenomena observed are mainly due to the properties of the nanometer-sized Bi particles themselves or support-independent interface properties.

The magnetic and electric fields created by the electron beam are negligible. The electric field in the high current density beam is approximately 1 V m^{-1}, whilst the magnetic field is calculated to be approximately 10^{-8} T under the same conditions.

The origin of the phase transitions is summarized in Figure 5 c and is discussed further here. In the following let Q be the heat flow. Q_{beam} is the heat flow into the particle produced by the electron beam and $Q_{interface}$ is the heat flow from the Bi particle to the support and away from the "hot spot".

Low electron-beam intensity ($<6\times10^3$ A m^{-2}): Even at this low beam intensity Q_{beam} is higher than $Q_{interface}$, which is equal to the heat flow from solid bismuth to the support. The temperature in the bismuth particle therefore increases to above the melting temperature of Bi and the particle becomes liquid. The heat flow, $Q_{interface}$, from liquid Bi to the support is now higher than from solid Bi to the support, and the temperature decreases, the particle solidifies, $Q_{interface}$ decreases, and the whole thing starts over again.

Medium electron-beam intensity: When the electron-beam intensity is increased, Q_{beam} becomes larger than both the heat flow from solid Bi to the support and liquid Bi to the support, so the Bi particles cannot cool down after melting and therefore remain liquid.

High electron-beam intensity ($>4\times10^5$ A m^{-2}): Due to the ionization processes and poor electric conductance, charges can build up at the interface. These charges change the surface potential, which might stabilize the crystalline Bi clusters (surface energy/interface energy). The situation is now similar to that at low electron-beam intensity, but with a higher melting temperature for Bi. The transformations are reversible.

Decreasing the beam intensity again discharges the Bi particles as the current flow from the Bi particles to the support is slow but non-zero, and the effective melting temperature decreases to the original value.

The threshold currents are expected to be a function of the support temperature. However, the temperature difference between room temperature and the melting temperature of Bi is too small to give consistent results.

The reversible phase transitions observed for nanometer-sized Bi particles under electron-beam irradiation in a transmission electron microscope can be explained by heating due to inelastic scattering of the electrons and charging effects of the small particles. The build-up of charge of

the Bi particles alters the surface tension, thereby stabilizing the solid phase and resulting in a higher effective melting temperature under intense electron beam irradiation, which leads to the solidification of the Bi particles at high beam-current density.

Experimental Section

The Bi nanoparticles used for our studies were supported on different materials. Bi supported on vanadium phosphorus oxide (VPO) was prepared using Bi-enriched VPO samples designed for butane oxidation[16] dispersed on carbon-coated Cu grids as starting material. The VPO samples are extremely sensitive to the electron beam in the TEM and lead to the formation of nanometer-sized Bi particles. These Bi particles are observed to migrate toward the surface of the oxide or even to the supporting carbon film. The size of the Bi particles is in the range 4-10 nm.

A fine powder of Bi was dispersed on carbon-coated Cu grids. Electron irradiation in the electron microscope produced 5-10-nm Bi grains at the surface of the Bi agglomerates as well as on the carbon film.

The samples were studied with a Philips CM 200 FEG electron microscope equipped with a Gatan Image Filter. The current densities used in the present experiments were in the region 5.0×10^{3}-5.0×10^{5} A m^{-2}.

References

1 X. Wang, H. Chen, *Mater. Chem. Phys.* 2002, **75**, 2.
2 Z. Yue, J. Zhou, X. Wang, Z. Gui, L. Li, *J. Eur. Ceram. Soc.* 2003, **23**, 189.
3 Z. Zhu, Y. Gao, X. Z. Che, Y. Q. Yang, C. Y. Chung, *J. Alloys Compd.* 2002, **330-332**, 708.
4 D. B. Williams, C. B. Carter, *Transmission Electron Microscopy*, Plenum Press, New York, 1996.
5 R. F. Egerton, P. Li, M. Malac, *Micron* 2004, **35**, 399.
6 F. Banhart, P. M. Ajayan, *Nature* 1996, **382**, 433.
7 F. Banhart, *J. Appl. Phys.* 1997, **81**, 3440.
8 Z. L. Wang, P. Poncharal, W. A. de Heer, *J. Phys. Chem. Solids* 2000, **61**, 1025.
9 G. Fuchs, M. Treilleux, F. S. Aires, B. Cabaud, A. Hoareau, P. Melinon, *Philos. Mag. A* 1990, **61**, 45.
10 P. Williams, *Appl. Phys. Lett.* 1987, **50**, 1760.
11 Y. Lereah, R. Kofman, J. M. Pénisson, G. Deutscher, P. Cheyssac, T. B. David, A. Bourret, *Philos. Mag. B* 2001, **11**, 1801.
12 P. A. Buffat, *Philos. Trans. R. Soc. London, Ser. A* 2003, **361**, 291.
13 M. Tanaka, M. Takeguchi, K. Furuya, *Micron* 2002, **33**, 441.
14 T. Ben-David, Y. Lereah, G. Deutscher, J. M. Penisson, A. Bourret, R. Kofman, P. Cheyssac, *Phys. Rev. Lett.* 1997, **78**, 2585.
15 K. Lu, Z. H. Jin, *Curr. Opin. Solid State Mater. Sci.* 2001, **5**, 39.
16 I. Ayub, D. S. Su, M. Willinger, A. Kharlamov, L. Ushkalov, V. A. Zazhigalov, N. Kirilova, R. Schlögl, *Phys. Chem. Chem. Phys.* 2003, **5**, 970.
17 S. Bernal, F. J. Botana, J. J. Calvino, C. López-Cartes, J. A. Pérez-Omil, J. M. Rodríguez-Izquierdo, *Ultramicroscopy* 1998, **72**, 135.
18 P. Stadelmann, *Ultramicroscopy* 1987, **21**, 131.
19 M. Treilleux, G. Fuchs, C. Montandon, F. S. Aires, P. Melinon, B. Cabaud, A. Hoareau, *Philos. Mag. A* 1993, **67**, 1071.
20 M. Treilleux, G. Fuchs, F. S. Aires, P. Melinon, A. Hoareau, B. Cabaud, *Z. Phys. D* 1991, **20**, 263.
21 V. P. Skripov, V. P. Koverda, V. N. Skokov, *Phys. Status Solidi A* 1981, **66**, 109.
22 L. H. Liang, J. C. Li, Q. Jiang, *Physica B* 2002, **322**, 188.
23 V. B. Storozhev, *Surf. Sci.* 1998, **397**, 170.
24 N. W. Ashcroft, N. D. Mermin, *Solid State Physics*, Saunders College Publishing, New York, 1976.
25 G. E. Smith, G. A. Baraff, J. M. Rowell, *Phys. Rev.* 1964, **135**, A 1118.
26 J. Cazaux, *Ultramicroscopy* 1995, **60**, 411.
27 J. G. Che, C. T. Chan, *Phys. Rev. B* 2003, **67**, 125411.
28 A. Y. Lozovoi, A. Alavi, *Phys. Rev. B* 2003, **68**, 245416.